Computers and Concrete, Vol. 2, No. 1 (2005) 55-77
DOI: http://dx.doi.org/10.12989/cac.2005.2.1.055

Closed form interaction surfaces for nonlinear design codes of RC columns with MC 90

M. H. F. M. Barros† and C. C. Ferreira‡

Civil Engineering Department, F. C. T., University of Coimbra, Polo II, 3030 Coimbra, Portugal

A. F. M. Barros‡†

IDMEC/IST, Mechanical Engineering Department, I. S. T., Lisbon, Portugal

Abstract. The closed form solution of the equilibrium equations in the ultimate design of reinforced concrete sections under biaxial bending is presented. The stresses in the materials are described by the Model Code 1990 equations. Computation of the integral equations is performed generally in terms of all variables. The deformed shape of the section in the ultimate conditions is defined by Heaviside functions. The procedure is convenient for the use of mathematical manipulation programs and the results are easily included into nonlinear analysis codes. The equations developed for rectangular sections can be applied for other sections, such as T, L, I for instance, by decomposition into rectangles. Numerical examples of the developed model for rectangular sections and composed sections are included.

Keywords: biaxial bending; closed form; nonlinear design code; heaviside functions; reinforced concrete; model code 1990.

1. Introduction

Ultimate design of reinforced concrete columns under biaxial bending and axial load is a complex problem due to the variation of the position of the neutral axis, defined by two independent variables. The ultimate condition for concrete sections is defined by the maximum strain in concrete or in steel. There are abacus that solve this problem in the case of simple shapes of sections, such as the rectangular section, with the parabola-rectangle stress diagram or the rectangular stress diagram (rsd) for concrete. The ultimate strain in concrete, in the equation indicated in the Model Code 1990 (MC90), depends on the concrete class. The stress-strain relation indicated in the MC90 is valid for short term loading and considers a descending branch after the peak stress. This relation is also dependent on the concrete grade and the differences to the previous laws increase with the quality of the concrete. Since the actual design codes are not yet prepared for this law, the present work develops the necessary equilibrium equations for the preparation of new design abacus. Recent works using parabola rectangle constitutive equation, solve the integrals by approximate methods, such as in Rodriguez (1999) and Fafitis (2001). Rodriguez (1999) performs the integration by

† Associate Professor, Corresponding Author, E-mail : hbarros@dec.uc.pt
‡ Auxiliar Professor, carla@dec.uc.pt
‡† Auxiliar Professor, melaopc@alfa.ist.utl.pt

dividing the compression zone into small rectangles. Fafitis (2001) makes the numerical integration by the Gauss quadrature. A more recent work by Bonet (2002) uses Gauss quadrature and the MC90 equation.

These numerical methods are implemented into computer codes but have the great disadvantage of depending on the number of integration points and dimension of the mesh. The solution obtained is not an exact solution and all numerical solutions have increasing computer costs when the mesh is refined.

The advantages of the present work are the following:

- the use of Model Code 1990 equation;
- the exact integration is obtained using MAPLE;
- the rectangular section is defined by its vertices;
- other sections, such as T, I or L can be considered by decomposing into small number of elementary rectangles;
- Heaviside functions are used in the definition of the rupture of the section, as in Barros, *et al.* (2004).

The objective of this work is to present the analytical formulation of the biaxial bending moment diagrams with the Model Code 1990 concrete stress-strain relation. These equations can be extended to reinforced concrete sections composed by rectangles. Examples of interaction diagrams are presented for rectangular and other reinforced concrete sections under biaxial bending.

The model developed is general and creep is taken into consideration in a simplified way by a reduction in the maximum strength. Confining effects can be included by modifying the input parameters in the relevant equations.

2. Geometric properties of the section

The sections considered in the present work can have any shape since they can be decomposed into rectangles. These are the cases of the sections represented in Fig. 1.

The elementary rectangle and the reinforcement are represented in Fig. 2. The dimensions are the width b, the height h and the concrete cover a. Reinforcement area is considered distributed uniformly along each side, being equal to A_1, A_2, A_3 and A_4, that is:

$$A_1 = a_1(h-2a);\quad A_2 = a_2(b-2a);\quad A_3 = a_3(h-2a);\quad A_4 = a_4(b-2a).$$

where a_1, a_2, a_3 and a_4 are the thickness of equivalent rectangles, as represented in Fig. 2.

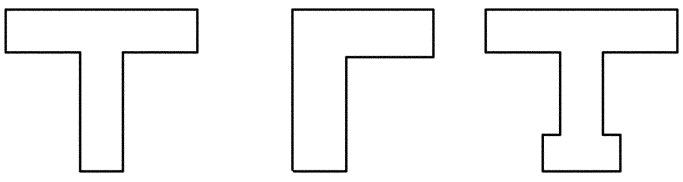

Fig. 1 Shape of the possible sections

3. Concrete stresses in compression

The constitutive relation used in the present work is indicated in the MC 90. This equation depends on the strength class of the concrete, defines the strength σ_c in terms of the strain ε, and is given by the following relation:

$$\sigma_c = 0.850 \frac{\left(\frac{E_c}{E_{c1}} \frac{\varepsilon}{\varepsilon_{c1}} + \frac{\varepsilon^2}{\varepsilon_{c1}^2} \right) f_{cd}}{1 - \left(\frac{E_c}{E_{c1}} - 2 \right) \frac{\varepsilon}{\varepsilon_{c1}}} \tag{1}$$

where f_{cd} is the maximum value of the stress and ε_{c1} (=0.0022) the corresponding strain in module. The remaining parameters are the elasticity modulus at the origin E_c and the secant elasticity modulus E_{c1} at the peak stress f_{cd}. The compressive strains ε are negative and so are the stresses σ_c. Fig. 3 represents Eq. (1) and parabola-rectangle law given by CEB (1982), for the classes of

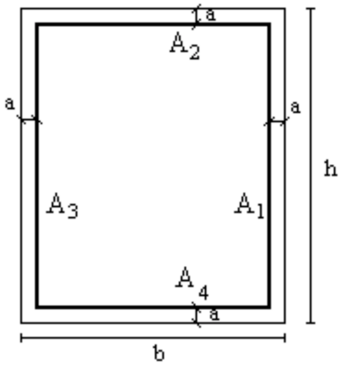

Fig. 2 Geometry of the section with reinforcing steel

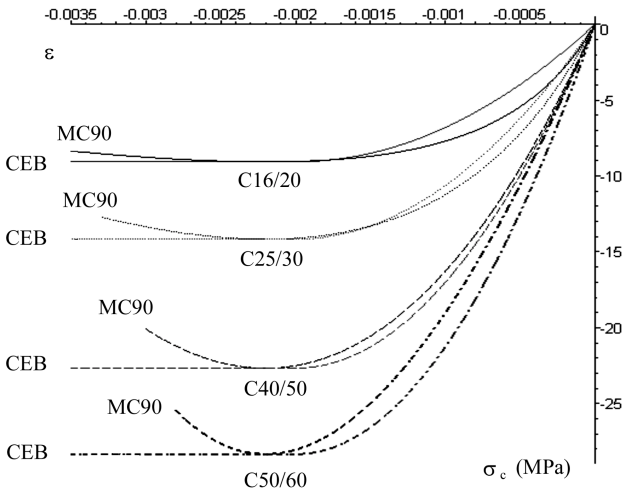

Fig. 3 Stress strain diagrams for different concrete classes

Table 1 Mechanical properties for concrete C16/20, C25/30, C40/50 and C50/60

	C16/20	C25/30	C40/50	C50/60
$E_{c,nom}$ (Gpa)	27.50	30.50	35.00	37.00
$E_c = E_{c,nom}/1.5$ (Gpa)	18.33	20.33	23.33	24.66
$f_{cd} = f_{ck}/1.5$ (Mpa)	10.67	16.67	26.67	33.33
ε_{cu}	0.0035	0.0033	0.0030	0.0028
$E_c/E_{c1} = 1.1E_c\ \varepsilon_{c1}/f_{cd}$	4.16	2.95	2.12	1.79

concrete which are resumed in Table 1.

In this work the rectangular stress diagram (rsd) for compressive stresses in concrete, suggested by the CEB-FIP 1990 in the case of complex shape sections, is also implemented and used in the numerical examples.

4. Constitutive relation of the steel

The constitutive relation of the steel is composed by an elastic behaviour followed by perfect plasticity. The elastic modulus of the steel is E_s and the design yield stress is f_{syd}. The steel stress σ_s is defined by a parametric function, in terms of the strain ε_s, that is:

$$\sigma_s = \begin{cases} -f_{syd} & \varepsilon_s \le -\dfrac{f_{syd}}{E_s} \\ E_s\varepsilon_s & -\dfrac{f_{syd}}{E_s} \le \varepsilon_s \le \dfrac{f_{syd}}{E_s} \\ f_{syd} & \dfrac{f_{syd}}{E_s} \le \varepsilon_s \end{cases} \tag{2}$$

In the case of S400 steel these values are: E_s=200000MPa and f_{syd}= 400/1.15MPa. The corresponding diagram is plotted in Fig. 4.

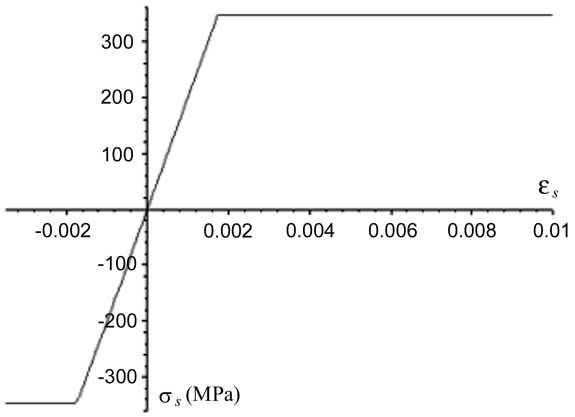

Fig. 4 Stress strain diagram for S400 steel

5. Section design

The rupture of the section may occur either in concrete or in steel being uniquely defined by the position of the neutral axis X indicated in Fig. 5. This position is defined by the variable a given by:

$$\alpha = \frac{X}{d} \tag{3}$$

where d is the effective height of the section, represented in Fig. 5. The rupture by the concrete, in the case of biaxial bending of a rectangular section, rotated by an angle β, is represented in Fig. 5(a). In this figure ε_c is the maximum strain in concrete equal to the rupture value $-\varepsilon_{cu}$. In the MC90 the ultimate strain in the concrete ε_{cu} is variable with the class of concrete and in the present model is considered in absolute value.

The rupture by the steel is represented in Fig. 5(b) where the strain in the more stressed steel ε_s is equal to the maximum 1%. This situation occurs for the small values of α and the maximum extension of the concrete is defined by

$$\varepsilon_c = 1\% \frac{\alpha}{\alpha - 1} \quad \text{if} \quad 0 \le \alpha \le \frac{\varepsilon_{cu}}{\varepsilon_{cu} + 1\%} \tag{4}$$

The rupture by the concrete is represented in Fig. 5(a). This rupture occurs in the high values of α where ε_c is given by:

$$\varepsilon_c = -\varepsilon_{cu} \quad \text{if} \quad \frac{\varepsilon_{cu}}{\varepsilon_{cu} + 1\%} < \alpha < \infty \tag{5}$$

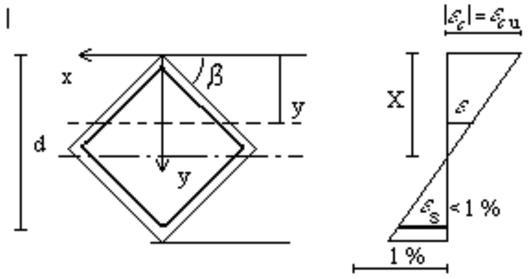

(a) Rupture by the concrete

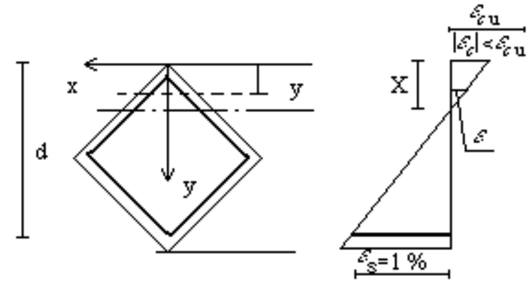

(b) Rupture by the steel

Fig. 5 Rupture by the concrete and the steel

These two relations are written in one equation by the use of Heaviside functions, as in Barros, *et al.* (2004), by the following equation:

$$\varepsilon_c = \frac{1}{100}\frac{\alpha}{\alpha-1} - H\left(\alpha - \frac{\varepsilon_{cu}}{\varepsilon_{cu}+1\%}\right)\left(\varepsilon_{cu} + \frac{\alpha}{100(\alpha-1)}\right) \tag{6}$$

A similar procedure is used in the maximum stressed steel in the definition of the strain ε_s. Rupture of steel will take place with small values of the non-dimensional variable α, Fig. 5(b), and the steel strain ε_s is given by

$$\varepsilon_s = 1\% \quad \text{if} \quad 0 \le \alpha \le \frac{\varepsilon_{cu}}{\varepsilon_{cu}+1\%} \tag{7}$$

For the rupture of concrete, Fig. 5(a), this strain is the following:

$$\varepsilon_s = -\varepsilon_{cu}\frac{\alpha-1}{\alpha} \quad \text{if} \quad \frac{\varepsilon_{cu}}{\varepsilon_{cu}+1\%} \le \alpha \le 1 \tag{8}$$

The strain in the steel ε_s is defined by a unique equation with the Heaviside function by:

$$\varepsilon_s = \frac{1}{100} - H\left(\alpha - \frac{\varepsilon_{cu}}{\varepsilon_{cu}+1\%}\right)\left(\frac{1}{100} + \frac{\alpha-1}{\alpha}\varepsilon_{cu}\right) \tag{9}$$

6. Equilibrium conditions

6.1. Resulting force and bending moments in concrete

6.1.1. Constitutive equation of the MC90

The resulting force and bending moments due to concrete stresses are obtained by the integration of the stresses in the compressed zone, denoted as A_c, that is:

$$N_c = \int_{A_c} \sigma_c dA \tag{10a}$$

$$M_{cx} = \int_{A_c} \sigma_c y dA \tag{10b}$$

$$M_{cy} = \int_{A_c} \sigma_c x dA \tag{10c}$$

The force N_c is the resulting force in the compressed concrete, the values M_{cx} and M_{cy} are the biaxial bending moments due to concrete stresses given in Barros, *et al.* (2003) referred to the axes xy as indicated in Fig. 5.

In the cases of biaxial bending moment, the shape of the compression concrete zone A_c is function of the position of the neutral axis, defined in terms of two parameters. These parameters are the distance X to the more compressed fibre and the angle β to the horizontal, as shown in Fig. 6(a).

The dashed zone A_c is divided into different cases, depending on the X and β, in the following way:

- Case I (Fig. 6b) : $0 \le X \le b\sin\beta \wedge 0 \le X \le h\cos\beta$;

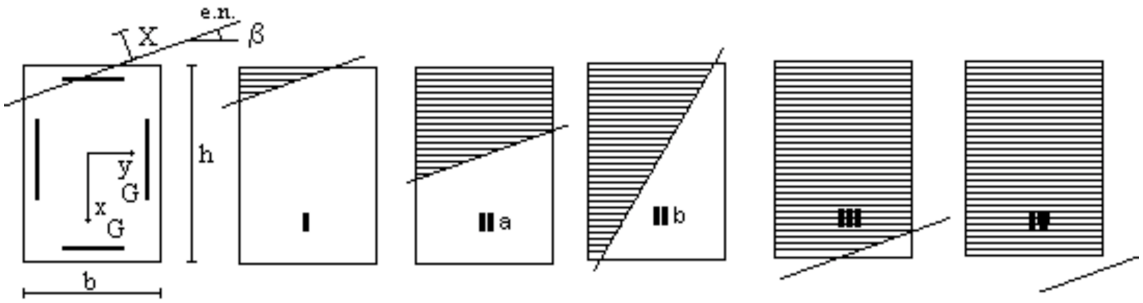

Fig. 6 Concrete compression zone A_c

- Case IIa (Fig. 6c) : $b\sin\beta \le X \le h\cos\beta$ if $b\sin\beta \le h\cos\beta$;
- Case IIb (Fig. 6d) : $h\cos\beta \le X \le b\sin\beta$ if $h\cos\beta \le X \le b\sin\beta$;
- Case III (Fig. 6e) : $b\sin\beta \le X \le b\sin\beta + h\cos\beta \wedge h\cos\beta \le X \le b\sin\beta + h\cos\beta$;
- Case IV (Fig. 6f) : $b\sin\beta + h\cos\beta \le X$.

The area integrals of the stress in the concrete defined by the MC90 (1) in the cases I to IV, respectively denoted by N_{c1}, N_{c2a}, N_{c2b}, N_{c3}, and N_{c4}, were developed in Barros, *et al.* (2003). The results are resumed in Annex I. Axial force N_c integrated in the variable domain is transformed into the addition of the cases multiplied by Heaviside functions, that is:

$$\begin{aligned} N_c \;=\; & N_{c1}H(h\cos\beta - X)H(X)H(b\sin\beta - X) + \\ & + N_{c2a}H(b\sin\beta - X)H(X - h\cos\beta)H(X) + \\ & + N_{c3}H(b\sin\beta + h\cos\beta - X)H(X - b\sin\beta)H(X - h\cos\beta)H(X) + \\ & + N_{c4}H(X - b\sin\beta - h\cos\beta)H(X) + \\ & + N_{c2b}H(h\cos\beta - X)H(X - b\sin\beta)H(X) \end{aligned} \tag{11}$$

Similar equations are obtained for the bending moments M_{cx} and M_{cy}.

6.1.2. Rectangular stress diagram

The previous integrals with the concrete stress defined by the rectangular stress diagram (rsd) are performed by defining the indicatrix function $I(x_G, y_G)$ equal to 1 in A_c and 0 outside A_c, that is:

$$I(x_G, y_G) \;=\; \begin{cases} 1 \;\; if \;\; (x_G, y_G) \in A_c \\ 0 \;\; if \;\; (x_G, y_G) \notin A_c \end{cases} \tag{12}$$

With this definition the integrals are calculated over the total area of the section A, becoming:

$$N_c \;=\; \int_A \sigma_c I(x_G, y_G)\, dA \tag{13a}$$

$$M_{cx} = \int_A \sigma_c y I(x_G, y_G) dA \tag{13b}$$

$$M_{cy} = \int_A \sigma_c x I(x_G, y_G) dA \tag{13c}$$

In the rectangular stress diagram (rsd) the stress in concrete is constant and σ_c in the previous equations is substituted by $0.80 f_{cd}$. The indicatrix function in this problem is defined by the following Heaviside function:

$$I(x_G, y_G) = H(X - y) \tag{14}$$

6.2. Resulting force and bending moments in steel

The axial load due to the steel and corresponding moments are calculated by the following integrations:

$$N_S = \oint \sigma_s ds \tag{15a}$$

$$M_{sxG} = \oint \sigma_s y G ds \tag{15b}$$

$$M_{syG} = \oint \sigma_s x G ds \tag{15c}$$

Since the stress σ_s is constant in the fibres located at the same distance X, the integration is performed with the following change in the variables, see Fig. 5:

$$y = X - \frac{X}{\varepsilon_c}\varepsilon; \quad dy = -\frac{X}{\varepsilon_c} d\varepsilon \tag{16}$$

The values of the expressions 15 (a), (b) and (c) are calculated relatively to the four sides of steel termed A_1, A_2, A_3 and A_4 in the Fig. 7, giving the following results:

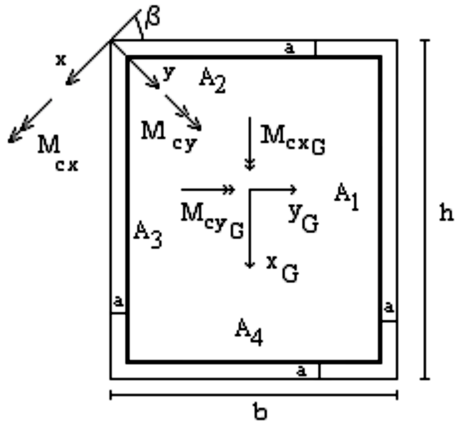

Fig. 7 Coordinate system change in the concrete biaxial bending moments

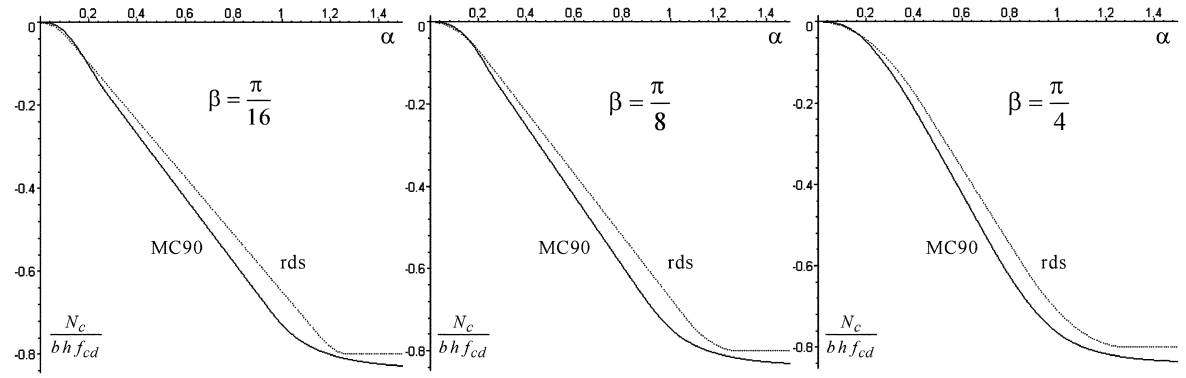

(a) C16/20 concrete class

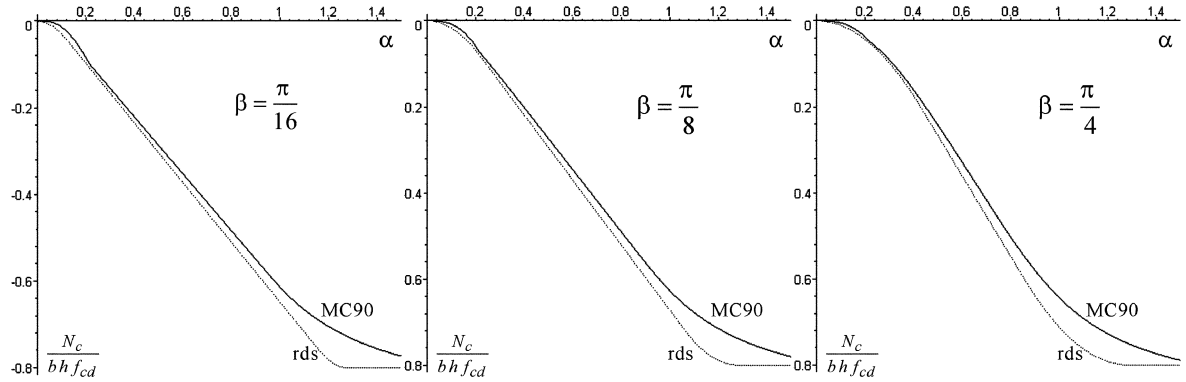

(b) C50/60 concrete class

Fig. 8 Concrete axial force variation with neutral axis depth

$$N_s = \sum_{i=1}^{4} F_i \tag{17a}$$

$$M_{sxG} = \left(\frac{b}{2} - a\right)(F_1 - F_3) - dF_2 - dF_4 \tag{17b}$$

$$M_{syG} = \left(a - \frac{h}{2}\right)(F_4 - F_2) + dF_1 + dF_3 \tag{17 c}$$

where the F_i and dF_i are indicated in Annex II.

6.3. Equilibrium equations for the axial force and bending moments

The equilibrium of the stresses applied to the section in terms of total force N and biaxial bending moments M_{xG} and M_{yG} are given respectively by:

$$N = N_c + N_s \tag{18a}$$

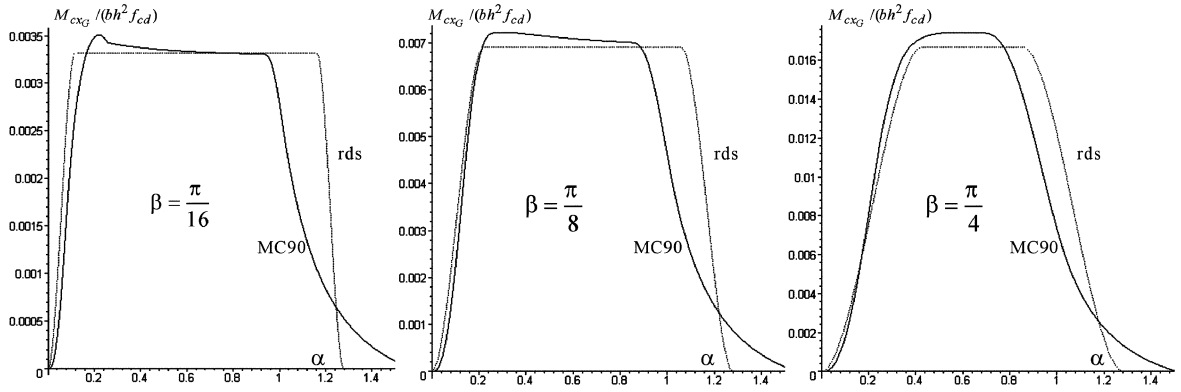

(a) C16/20 concrete class

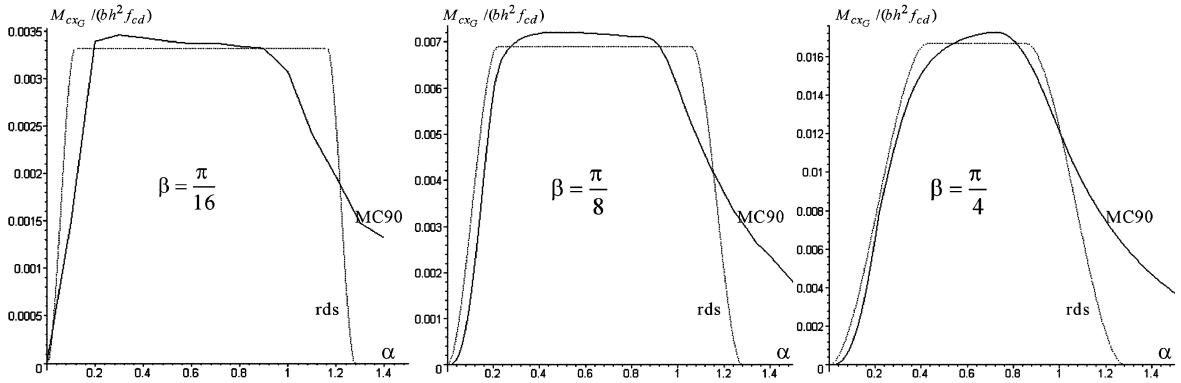

(b) C50/60 concrete class

Fig. 9 Concrete reduced bending moment M_{cxG} variation with neutral axis depth

$$M_{xG} = M_{cxG} + M_{sxG} \tag{18b}$$

$$M_{yG} = M_{cyG} + M_{syG} \tag{18c}$$

where the bending moments due to the concrete stresses must be changed into the global system, that is M_{cxG} and M_{cyG} in Fig. 7. The results are the following:

$$M_{cxG} = M_{cx}\sin(\beta) + M_{cy}\cos(\beta) - N_c b/2 \tag{19a}$$

$$M_{cyG} = -M_{cx}\cos(\beta) + M_{cy}\sin(\beta) + N_c h/2 \tag{19b}$$

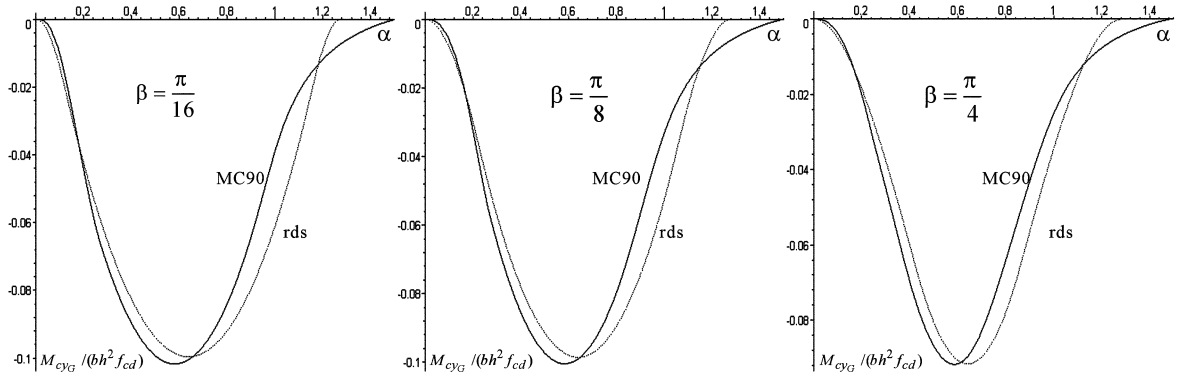

(a) C16/20 concrete class

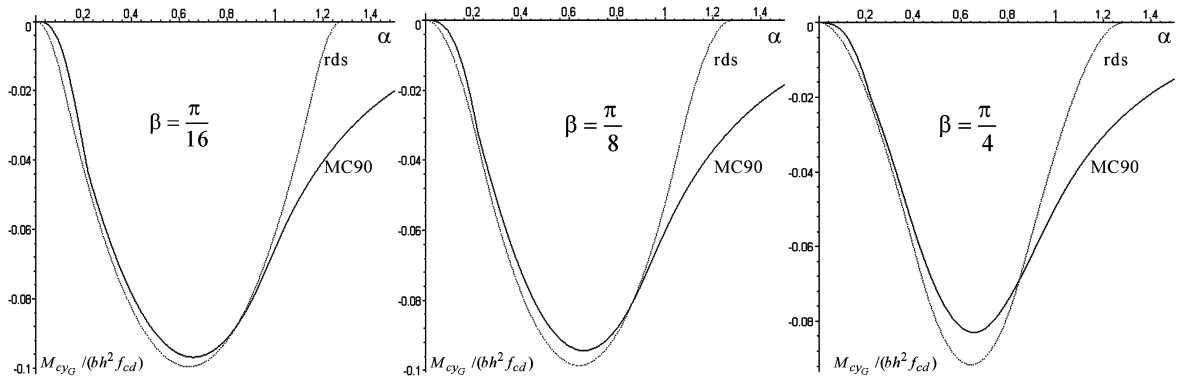

(b) C50/60 concrete class

Fig. 10 Concrete reduced bending moment M_{cyG} variation with neutral axis depth

7. Numerical examples

7.1. Axial force in concrete and steel in a rectangular section

To exemplify the resultant force in the concrete, Eqs. 10(a), (b) and (c), a rectangular section with height 2.0 m and width 1.0 m is considered. In Figs. 8(a) to (f), the values of reduced compressive force $N_c/(bhf_{cd})$ are plotted in function of neutral axis depth, α given by (3). Three values of the neutral axis inclination ($\beta=\pi/16$, $\beta=\pi/8$, $\beta=\pi/4$) and two classes of concrete, C16/20 and C50/60, are considered. The reduced force obtained with the rectangular stress diagram (rsd) is also plotted and it can be compared with the value computed through MC90 equation, signalled by MC90 in Figs. 8.

In Figs. 9(a), 9(b) and Figs. 10(a), 10(b), the reduced bending moment $M_{cxG}/(bh^2f_{cd})$ and $M_{cyG}/(bh^2f_{cd})$ are also plotted for the same values of β, classes of concrete and considering the two constitutive relations that are the rectangular stress diagram (rsd) and the MC90 equation. These diagrams show that the differences in the two models increase with the concrete grade and also when the section is all compressed, near $\alpha=1$. Nevertheless the changes in β are not relevant.

Fig. 11 exemplifies the computations of the axial force N_s and bending moment M_{syG} variation in steel with neutral axis depth α, for the ultimate strains values ε_{cu} corresponding to the four classes

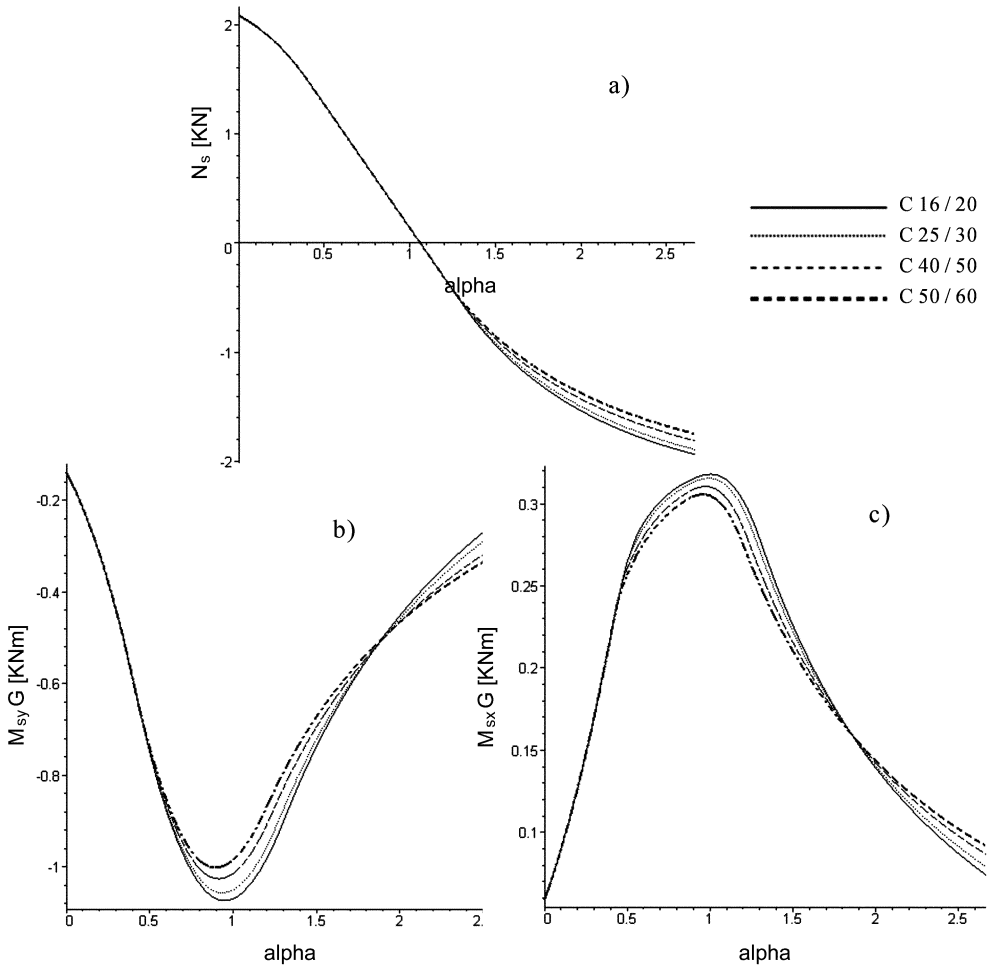

Fig. 11 Axial force and bending moment M_{syG} and M_{sxG} variation in steel

of concrete, related in Table 1. The curves obtained by the use of the expressions 17(a) and (c) and using the relevant definitions in Annex II are plotted in Fig. 11. The angle β considered is $\pi/4$. The other geometric properties of the section are the following: b=1 m, h=2 m, a_1=a_2=a_3=a_4=0.001 m, a=0.05 m, E_s=200000Mpa and f_{syd}= 400MPa.

It can be observed in this figure that the concrete grade also affects the force and moments in the steel. Fig. 11a) shows that increasing the concrete grade the axial force decrease in absolute value.

7.2. Interaction surfaces in biaxial bending of a rectangular section

A section with $0.40 \times 0.40\ \text{m}^2$ made in concrete C16/20 ($\varepsilon_{cu} = 0.0035$ and $f_{cd} = 10.67$Mpa) is reinforced with different steel area. The cover of steel is a=0.04 m. The steel class S400 with $f_{syd} = 400/1.15$Mpa is uniformly distributed along the sides of the section. Four different reinforcing bars are considered, 4ϕ16, 4ϕ20, 8ϕ16 and 8ϕ20. Interaction bending moment diagrams for a constant

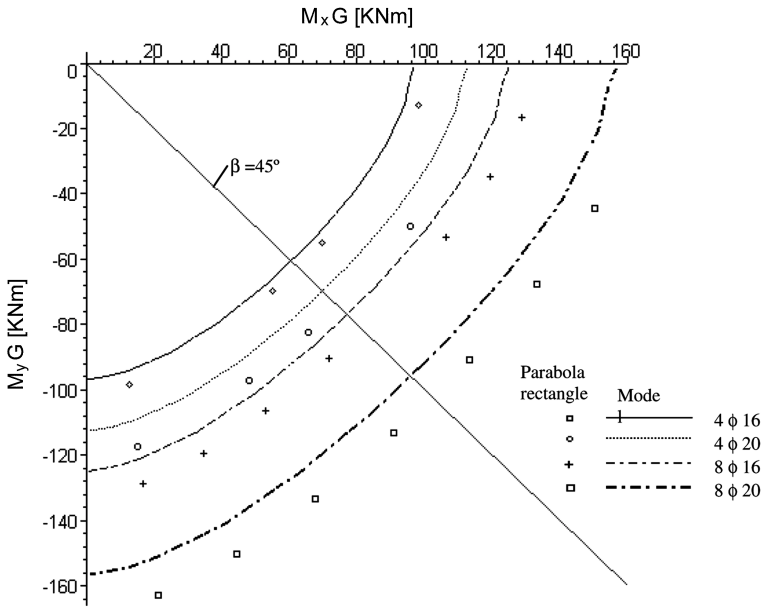

Fig. 12 Interaction $M_{x_G} - M_{y_G}$

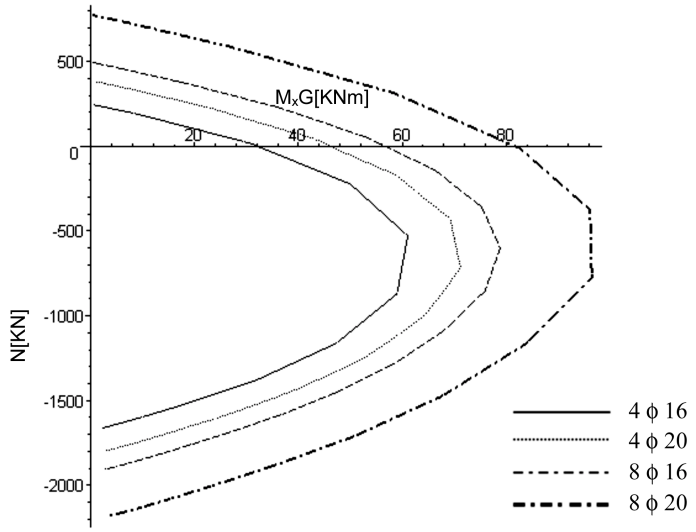

Fig. 13 Interaction $N \leftrightarrow M_{x_G}$ in the present model for β=45°

axial load $N = -683$KNare represented in Fig. 12. The present model is compared to parabola-rectangle law given by CEB (1982). The present results are more conservative, since the resistant bending moments are smaller than those with the parabola-rectangle. The interaction diagram $N \leftrightarrow M_{x_G}$, for $M_{x_G} = -M_{y_G}$ (that is b=45°), is also represented in Fig. 13 for different steel areas.

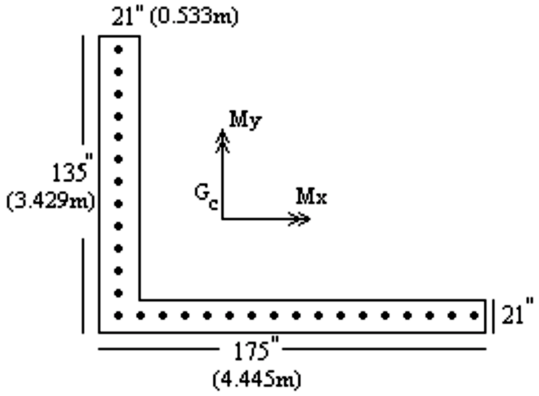

Fig. 14 Geometry of corner shear wall

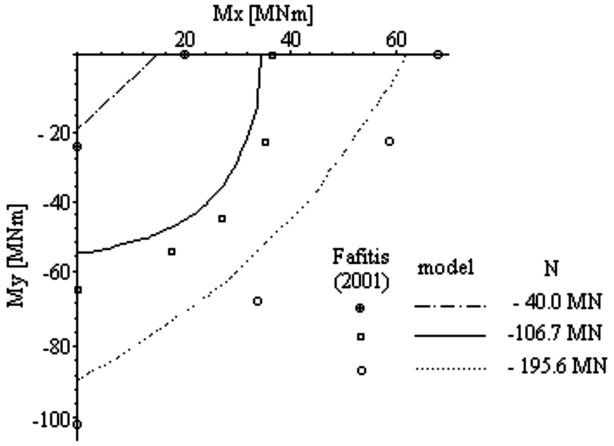

Fig. 15(a) Interaction M_x–M_y (MNm) for a corner shear wall

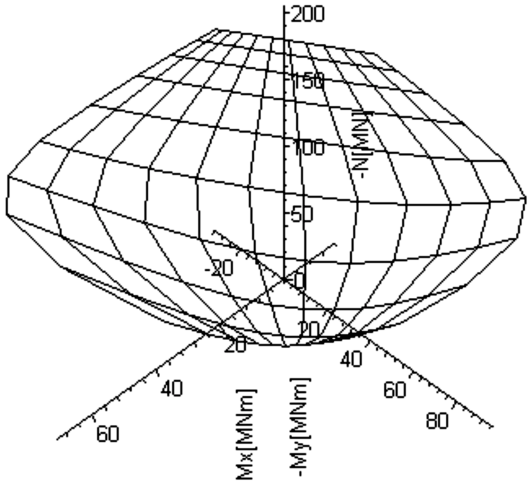

Fig. 15(b) Interaction surface of the corner shear wall

7.3. Interaction surfaces of a corner shear wall in biaxial bending

The present model is used in the analysis of the corner shear wall presented in Fafitis (2001). The geometry of the wall with 29 steel bars of 1" (0.0254 m) diameter is indicated in Fig. 14. The concrete strength is f_{cd} = 9000Psi (62.07MPa), that is concrete class C50/60, an the steel strength is f_{sy} = 60000Psi (413.80MPa). The bending moments are calculated at the gravity center G_c of the concrete section. The results are presented in Fig. 15. In Fig. 15(a) the interaction $M_{x_G} - M_{y_G}$ diagrams are plotted for N = –9000Kips(–40.0MN), N = –24000Kips (–106.7MN) and N = –44000Kips (–195.6MN) obtained with present model. The results by Fafitis (2001) are also represented. The model developed is more conservative than the results obtained by Fafitis (2001). In Fig. 15(b) the interaction surface is represented.

Using MAPLE the quality of the interaction abacus is dependent on the number of points used in the definition of the figures. In the computation of the present abacus this number is small because the symbolic language is not the more appropriate for intensive computation. The change to FORTRAN language can improve the solution.

8. Conclusions

In the present work the expressions for the evaluation of the axial load and biaxial bending moment in a reinforced concrete section are derived analytically with the mathematical program MAPLE. This program is very convenient for the section design due to the quick and easy implementation.

The constitutive relation of the concrete under compression is described either by the MC90 equation or the rectangular constant diagram. The equations for the biaxial bending moment and axial force can be introduced into computer codes with the advantage of having the exact solution instead of approximated solutions. The equations deducted to rectangular sections can be applied into other sections, such as T, L, I or other, simply by decomposing them into small rectangles. These equations can also be used in the elaboration of tables or design abacus. The numerical examples consist of interaction diagrams for biaxial bending moment of different concrete sections. The results are compared to the CEB (1982) model and it is concluded that in the high strength concrete the present model can be more conservative in terms of the ultimate design.

Acknowledgements

Part of this work is developed within FCT, Fundacão Parava Ciência e Technologia Portuguese Minister of Science and Technology the Programa Operacional do Quadro Comunitário de Apoio (POCTI), and by FEDER, by grant POCTI /P/ECM/12126/1998/2001, Fase II.

References

ACI, American Concrete Institute (1995), "Building code requirements for structural concrete", *ACI*, 318-95, Detroit.

Barros, M. H. F. M., Barros A., Ferreira C. (2004), "Closed form solution of optimal design of rectangular reinforced concrete sections", *Eng. Comput.,* **21**(7), 761-776.
Barros, M. H. F. M., Ferreira, C. C., Barros, A. F. M. (2003), "Integração do diagrama de tensões de compressão do betão em flexão desviada usando a equação do", Construlink, www.construlink.com, **1** (3), 41-49.
Brondum-Nielsen, T. (1985), "Ultimate flexural capacity of cracked poligonal concrete sections under biaxial bending", *ACI Struct. J.*, **82**(6), 863-869.
Bonet, J. L., Miguel, P. F., Romero, M. L., Fernandez, M. A (2002), "A modified algorithm for reinforced concrete cross sections integration", *Proceedings of VI Int. Conf. Comput. Struct. Tech., Civil-Comp Press*, Scotland.
CEB-FIP Model Code 1990 (1991), Committee Euro-International du Beton, CEB Bulletin 203-204, 205 Thomas Telford.
CEB-FIP Manual on Bending and Compression (1982), Committee Euro-International du Beton, Boletim 141.
Dundar, C. (1990), "Concrete box sections under biaxial bending and axial load", *J. Struct. Eng.*, ASCE, **116**(3), 860-865.
Fafitis, A (2001), "Interaction surfaces for of reinforced concrete sections in biaxial bending", *J. Struct. Eng.*, ASCE, **127**(7), 840-846.
Hsu, C. T. T. (1989), "T-shaped reinforced concrete members under biaxial bending and axial compression", *ACI Struct. J.*, **86**(4), 460-468.
Rodriguez, J. A., Ochoa, J. D. A., (1999), "Biaxial interaction diagrams for short RC columns of any cross section", *J. Struct. Eng.,* ASCE, 125(6), 672-683.

ANNEX I

In the following expressions the ratio of elasticity modulus at the origin and the secant value is denoted by $E_{cc1}=E_c / E_{c1}$. Axial forces N_{c1} (Fig. 6b), N_{c2a} (Fig. 6c), N_{c2b} (Fig. 6d), N_{c3} (Fig. 6e) and N_{c4} (Fig. 6f) are given by:

$$N_{c_1} = \frac{7}{120} f_{cd} X^3 (6\varepsilon_{c1}^3 (1-E_{cc1})^2 (k1-k2) - \varepsilon_c^3 (E_{cc1}-2)^3 + 6\varepsilon_{c1}^2 \varepsilon_c (1-E_{cc1})^2 (E_{cc1}-2)(k2-k1) - 3\varepsilon_c^2 \varepsilon_{c1} (E_{cc1}-2)^2 (1-E_{cc1})^2) / k14$$

$$\begin{aligned} N_{c_{2a}} = & -\frac{17}{40} b f_{cd} (\varepsilon_c^2 (E_{cc1}-2)^2 (X - b\sin(\beta))^2 - 2X^2 \varepsilon_{c1}^2 (E_{cc1}-1)^2 (k2-k6) \\ & -2\varepsilon_{c1}\varepsilon_c (E_{cc1}-2)(E_{cc1}-1)^2 (X^2 - b\sin(\beta)X) / (\cos(\beta) X \varepsilon_{c1} (E_{cc1}-2)^3 \varepsilon_c) \\ & -\frac{17}{120} f_{cd} (3Xb^2 \sin(\beta)^2 (\varepsilon_c^3 (E_{cc1}-2)^3 + \varepsilon_{c1}\varepsilon_c^2 (E_{cc1}-2)^2 (E_{cc1}-1)^2) \\ & +6\varepsilon_{c1}^2 \varepsilon_c (E_{cc1}-2)(E_{cc1}-1)^2 (X^3 (k1-k6) - X^2 b\sin(\beta)) \\ & -2\varepsilon_c^3 b^3 \sin(\beta)^3 (E_{cc1}-2)^3 + 6\varepsilon_{c1}^3 X^3 (E_{cc1}-1)^2 (k6-k1) / k14 \end{aligned}$$

$$N_{c_{2b}} = -\frac{17}{40} hf_{cd}\,(\varepsilon_c^2(E_{cc1}-2)^2(X-h\cos(\beta))^2 - 2X^2\varepsilon_{c1}^2(E_{cc1}-1)^2(k2-k3)$$
$$+2X\varepsilon_{c1}\varepsilon_c(E_{cc1}-2)(E_{cc1}-1)^2(X-h\cos(\beta)))/(\sin(\beta)X\varepsilon_{c1}(E_{cc1}-2)^3\varepsilon_c)$$
$$-\frac{17}{120} f_{cd}(3Xh^2\cos(\beta)^2(\varepsilon_c^3(E_{cc1}-2)^3 + \varepsilon_{c1}\varepsilon_c^2(E_{cc1}-2)^2(E_{cc1}-1)^2)$$
$$+6\varepsilon_{c1}^2\varepsilon_c(E_{cc1}-2)(E_{cc1}-1)^2(X^3(k1-k3)-X^2h\cos(\beta)) - 2\varepsilon_c^3h^3\cos(\beta)^3$$
$$(E_{cc1}-2)^3 + 6\varepsilon_{c1}^3X^3(E_{cc1}-1)^2(k3-k1)/k14$$

$$N_{c_3} = N_{c_{2a}} - \frac{17}{120} f_{cd}(6\varepsilon_{c1}^2\varepsilon_cX^2(E_{cc1}-2)(E_{cc1}-1)^2(1+k2-k3)(X-h\cos(\beta))$$
$$-3X\varepsilon_{c1}\varepsilon_c^2(E_{cc1}-2)^2(E_{cc1}-1)^2(X-h\cos(\beta))^2$$
$$+\varepsilon_c^3(E_{cc1}-2)^3(3h\cos(\beta)X^2 - X^3 + h^3\cos(\beta)^3 - 3h^2\cos(\beta)^2X)$$
$$-6\varepsilon_{c1}^3X^3(E_{cc1}-1)^2(k2-k3)/k14$$

$$N_{c_4} = N_{c2a} + \frac{17}{40} f_{cd}b(2(E_{cc1}-1)^2X^2\varepsilon_{c1}^2(k7-k2) + X\varepsilon_c\varepsilon_{c1}(E_{cc1}-2)(X$$
$$-b\sin(\beta)-h\cos(\beta))) + \varepsilon_c^2(E_{cc1}-2)^2((b\sin(\beta)+h\cos(\beta))^2 + X^2$$
$$-2h\cos(\beta)X - 2Xb\sin(\beta)))/(\cos(\beta)X\varepsilon_{c1}\varepsilon_c(E_{cc1}-2)^3) - \frac{17}{120} f_{cd}$$
$$(6X^2\varepsilon_{c1}^2\varepsilon_c(E_{cc1}-1)^2(E_{cc1}-2)((k7-k3)(X+b\sin(\beta))-h\cos(\beta))$$
$$+\varepsilon_c^3b^2\sin(\beta)^2(E_{cc1}-2)^3(3h\cos(\beta)-3X+2b\sin(\beta)) - 6X^3\varepsilon_{c1}^3$$
$$(E_{cc1}-1)^2(k7-k3) - 3\varepsilon_c^2X\varepsilon_{c1}b^2\sin(\beta)^2(E_{cc1}-1)^2(E_{cc1}-2)^2/k14$$

Bending moments M_{cx1} and M_{cy1} in Fig. 6(b); M_{cx2a} and M_{cy2a} in Fig. 6(c); M_{cx2b} and M_{cy2b} in Fig. 6(d); M_{cx3} and M_{cy3} in Fig. 6(e); M_{cx4} and M_{cy4} in Fig. 6(f) are the following:

$$M_{cx1} = -\frac{17}{240} f_{cd}X^4\varepsilon_c^4(E_{cc1}-2)^4 + 12\varepsilon_{c1}^4(E_{cc1}-1)^2(k1-k2) + (E_{cc1}-1)^2$$
$$(\varepsilon_{c1}^2\varepsilon_c^2(E_{cc1}-2)^2(12(k1-k2)-18) + \varepsilon_{c1}^3\varepsilon_c(E_{cc1}-2)(12-24(k1-k2))$$
$$+4\varepsilon_{c1}\varepsilon_c^3(E_{cc1}-2)^3))/k15$$

$$M_{cy1} = M_{cx1}(\sin(\beta)^2 - \cos(\beta)^2)/(\cos(\beta)\sin(\beta))$$

$$M_{cx2a} = -\frac{17}{120} b f_{cd} k10 / (\cos(\beta)(E_{cc1}-2)^4 X \varepsilon_c^2 \varepsilon_{c1}) - \frac{17}{240} f_{cd} k11$$

$$\begin{aligned} M_{cy2a} = {} & \frac{17}{240} f_{cd} b (2k10\sin(\beta) + 6\varepsilon_c b X^2 \varepsilon_{c1}^2 (k2-k6)(E_{cc1}-2)(E_{cc1}-1)^2 \\ & -3\varepsilon_c^3 b (E_{cc1}-2)^3 (X - b\sin(\beta))^2 - 6\varepsilon_{c1}\varepsilon_c^2 (E_{cc1}-2)^2 (E_{cc1}-1)^2 \\ & (bX^2 - b^2 X \sin(\beta))) / (\varepsilon_{c1}\cos(\beta)^2 X \varepsilon_c^2 (E_{cc1}-2)^4) \\ & -\frac{17}{480} f_{cd} (\sin(\beta)^2 - \cos(\beta)^2) k11 / \sin(\beta)\cos(\beta) \end{aligned}$$

$$M_{cx2b} = -\frac{17}{120} h f_{cd} k4 / (\sin(\beta)(E_{cc1}-2)^4 X \varepsilon_c^2 \varepsilon_{c1}) - \frac{17}{240} f_{cd} k5$$

$$\begin{aligned} M_{cy2b} = {} & \frac{17}{240} f_{cd} h (2k4\cos(\beta) + 6\varepsilon_c h X^2 \varepsilon_{c1}^2 (k2-k3)(E_{cc1}-2)(E_{cc1}-1)^2 \\ & -3\varepsilon_c^3 h (E_{cc1}-2)^3 (X - h\cos(\beta))^2 - 6\varepsilon_{c1}\varepsilon_c^2 (E_{cc1}-2)^2 (E_{cc1}-1)^2 \\ & (hX^2 - h^2 X \cos(\beta))) / (\varepsilon_{c1}\sin(\beta)^2 X \varepsilon_c^2 (E_{cc1}-2)^4) \\ & -\frac{17}{480} f_{cd} (\sin(\beta)^2 - \cos(\beta)^2) k5 / \sin(\beta)\cos(\beta) \end{aligned}$$

$$\begin{aligned} M_{cx3} = {} & M_{cx2a} - \frac{17}{240} f_{cd} (12X^4 \varepsilon_{c1}^4 (E_{cc1}-1)^2 (k2-k3) + X^2 \varepsilon_{c1}^2 \varepsilon_c^2 (E_{cc1}-1)^2 (E_{cc1}-2)^2 \\ & (18X^2 + 6h^2\cos(\beta)^2 - 12Xh\cos(\beta)(k2-k3+2) + 12X^2(k2-k3)) \\ & +12\varepsilon_{c1}^3 \varepsilon_c (E_{cc1}-1)^2 (E_{cc1}-2)(X^3 h\cos(\beta)(k2-k3+1) - 2X^4(k2-k3) - X^4) \\ & +\varepsilon_c^4 (E_{cc1}-2)^4 (h^4\cos(\beta)^4 - X^4 + 2X^3 h\cos(\beta) - 2Xh^3\cos(\beta)^3) \\ & +\varepsilon_{c1}\varepsilon_c^3 (E_{cc1}-1)^2 (E_{cc1}-2)^3 (6X^3 h\cos(\beta) - 4X^4 - 2Xh^3\cos(\beta)^3)) / k15 \end{aligned}$$

$$\begin{aligned} M_{cy3} = {} & M_{cy2a} + \frac{17}{480} f_{cd} (\varepsilon_c^4 (E_{cc1}-2)^4 (4\cos(\beta)^3 X (hX^2 - \sin(\beta)^2 h^3 + 3) \\ & +h^4\cos(\beta)^4 (3\sin(\beta)^2 - 6) + 5\cos(\beta)^6 h^4 - 8Xh^3\cos(\beta)^5 - 6h^2\cos(\beta)^2 X^2 \\ & -X^4\cos(2\beta)) + \varepsilon_c^2 \varepsilon_{c1}^2 (E_{cc1}-2)^2 (E_{cc1}-1)^2 (12X^3\sin(\beta)^2 h\cos(\beta) + (6 \\ & +4(k2-k3))(3X^4\cos(2\beta)) - 6X^3\cos(\beta)^3 h) + X^2 h^2 \cos(\beta)^2 (6\sin(\beta)^2 \end{aligned}$$

$$+18\cos(\beta)^2 + 12(k2-k3))) + \varepsilon_c^3\varepsilon_{c1}(E_{cc1}-2)^3(E_{cc1}-1)^2(12\cos(\beta)^3hX^3$$

$$-12h^2\cos(\beta)^2X^2 - \cos(\beta)^3Xh^3(8\cos(\beta)^2 + 4\sin(\beta)^2 - 12) - 4X^4\cos(2\beta))$$

$$+\varepsilon_c\varepsilon_{c1}^3(E_{cc1}-2)(E_{cc1}-1)^2 24\cos(\beta)^3hX^3(k2-k3) + 12\cos(2\beta)X^3$$

$$(\cos(\beta)h - X - 2X(k2-k3))) + 12X^4\varepsilon_{c1}^4(E_{cc1}-1)^2\cos(2\beta)(k2-k3))$$
$$/(\sin(\beta)\cos(\beta)k15)$$

$$M_{cx4} = M_{cx2a} + \frac{17}{120}f_{cd}b(k12 + 6X^2\varepsilon_{c1}^2\varepsilon_c h\cos(\beta)(E_{cc1}-2)(E_{cc1}-1)^2$$

$$-\varepsilon_{c1}\varepsilon_c^2(E_{cc1}-2)^2(E_{cc1}-1)^2(3Xh^2\cos(\beta)^2 + 6Xb\sin(\beta)h\cos(\beta))$$

$$+\varepsilon_c^3(E_{cc1}-2)^3h\cos(\beta)(h\cos(\beta)(6b\sin(\beta) - 3X) + 6b^2\sin(\beta)^2$$

$$+2h^2\cos(\beta)^2 - 6Xb\sin(\beta)))/(\cos(\beta)X\varepsilon_{c1}\varepsilon_c^2(E_{cc1}-2)^4)$$

$$+\frac{17}{240}f_{cd}k13 - \frac{17}{240}f_{cd}(\varepsilon_c^4b^2\sin(\beta)^2h\cos(\beta)(E_{cc1}-2)^4(8b\sin(\beta) - 6X$$

$$+6h\cos(\beta)) + 6h\cos(\beta)(E_{cc1}-1)^2((k3-k7)(2X^3\varepsilon_c^2\varepsilon_{c1}^2(E_{cc1}-2)^2$$

$$-2X^3\varepsilon_{c1}^3\varepsilon_c(E_{cc1}-2)) - \varepsilon_c^3X\varepsilon_{c1}b^2\sin(\beta)^2((E_{cc1}-2)^3))/k15$$

$$M_{cy4} = M_{cy2a} + \frac{17}{240}f_{cd}b(2k12\sin(\beta) + 6\varepsilon_{c1}\varepsilon_c^2(E_{cc1}-2)^2(E_{cc1}-1)^2(X\sin(\beta)$$

$$(b^2 - h^2\cos(\beta)^2) - bX^2 + hXb\cos(\beta)(1 - 2\sin(\beta)^2)) + \varepsilon_c^3(E_{cc1}-2)^3(6\sin(\beta)$$

$$(X - h\cos(\beta))(b^2 - 2\cos(\beta)hb\sin(\beta)) + 12\cos(\beta)b^2\sin(\beta)^3h - 3b^3\sin(\beta)^2$$

$$-6\cos(\beta)^2Xh^2\sin(\beta) + 4\cos(\beta)^3h^3\sin(\beta) - 3b(X - h\cos(\beta))^2)$$

$$+X^2\varepsilon_{c1}^2\varepsilon_c(E_{cc1}-2)(E_{cc1}-1)^2(6b(k2-k7) + 12\cos(\beta)h\sin(\beta)))/(\varepsilon_{c1}$$

$$\cos(\beta)^2X\varepsilon_c^2(E_{cc1}-2)^4) - \frac{17}{480}f_{cd}(\cos(\beta)^2 - \sin(\beta)^2)k13/(\sin(\beta)\cos(\beta))$$

$$-\frac{17}{480}f_{cd}24X^3\varepsilon_{c1}^3\cos(\beta)^3h\varepsilon_c(E_{cc1}-2)(E_{cc1}-1)^2(k3-k7) - 12\sin(\beta)^4$$

$$\varepsilon_c^3X\varepsilon_{c1}b^2\cos(\beta)h(E_{cc1}-2)^3(E_{cc1}-1)^2 + 12X^2\varepsilon_{c1}^2\varepsilon_c^2(E_{cc1}-2)^2(E_{cc1}-1)^2$$

$$h\cos(\beta)(b\sin(\beta) + (k3-k7)(h\cos(\beta) - 2X\cos(\beta)^2)) + \varepsilon_c^4(E_{cc1}-2)^4(12bh^2$$

$$\sin(\beta)(\cos(\beta)^2 X + \cos(\beta)^5 h - \cos(\beta)^4 X - h\cos(\beta)^3) + h^2\cos(\beta)^2(18\sin(\beta)^4 b^2$$
$$-12\cos(\beta)^3 Xb) - 4\sin(\beta)^3\cos(\beta)^3(b^3 h - 3bh^3) - 6b^2h^2\sin(\beta)^4\cos(\beta)^2$$
$$+12h\cos(\beta)(b^3\sin(\beta)^5 - b^2\sin(\beta)^4 X)))/(\cos(\beta)\sin(\beta)k15)$$

Parameters K in these expressions are given by:

$$k1 = \ln(X\varepsilon_{c1} - \varepsilon_c E_{cc1} X + 2\varepsilon_c X)$$

$$k2 = \ln(X\varepsilon_{c1})$$

$$k3 = \ln(X\varepsilon_{c1} + \varepsilon_c(E_{cc1} - 2)(h\cos(\beta) - X))$$

$$k4 = 6\varepsilon_{c1}^2\varepsilon_c(E_{cc1} - 1)^2(E_{cc1} - 2)(X^2 h\cos(\beta) - X^3(1 - k3 + k2)) + 3\varepsilon_{c1}\varepsilon_c^2$$
$$(E_{cc1} - 1)^2(E_{cc1} - 2)^2(X^3 - Xh^2\cos(\beta)^2) + 6\varepsilon_{c1}^3 X^3(E_{cc1} - 1)^2(k2 - k3)$$
$$+\varepsilon_c^3(E_{cc1} - 2)^3(X^3 + 2h^3\cos(\beta)^3 - 3Xh^2\cos(\beta)^2)$$

$$k5 = (12X^4(k1 - k3)(E_{cc1} - 1)^2\varepsilon_{c1}^2(\varepsilon_{c1} - \varepsilon_c(E_{cc1} - 2))^2 - \varepsilon_{c1}^2\varepsilon_c^2(E_{cc1} - 2)^2$$
$$(E_{cc1} - 1)^2(12X^3 h\cos(\beta) + 6X^2 h^2\cos(\beta)^2) + \varepsilon_c^4(E_{cc1} - 2)^4(4Xh^3\cos(\beta)^3$$
$$-3h^4\cos(\beta)^4) + 12X^3\varepsilon_{c1}^3 h\cos(\beta)\varepsilon_c(E_{cc1} - 2)(E_{cc1} - 1)^2 + 4h^3\cos(\beta)^3\varepsilon_c^3$$
$$X\varepsilon_{c1}(E_{cc1} - 2)^3(E_{cc1} - 1)^2)/k15$$

$$k6 = \ln(X\varepsilon_{c1} + \varepsilon_c(E_{cc1} - 2)(b\sin(\beta) - X))$$

$$k7 = \ln(X\varepsilon_{c1} + \varepsilon_c(E_{cc1} - 2)(b\sin(\beta) + h\cos(\beta) - X))$$

$$k8 = 6\varepsilon_{c1}^2\varepsilon_c(E_{cc1} - 1)^2(E_{cc1} - 2)(X^2 h\cos(\beta) - X^3(1 - k7 + k2)) + 3\varepsilon_{c1}\varepsilon_c^2$$
$$(E_{cc1} - 1)^2(E_{cc1} - 2)^2(X^3 - Xh^2\cos(\beta)^2) + 6\varepsilon_{c1}^3 X^3(E_{cc1} - 1)^2(k2 - k7)$$
$$+\varepsilon_c^3(E_{cc1} - 2)^3(X^3 + 2h^3\cos(\beta)^3 - 3Xh^2\cos(\beta)^2)$$

$$k9 = (12X^4(k6 - k7)(E_{cc1} - 1)^2\varepsilon_{c1}^2(\varepsilon_{c1} - \varepsilon_c(E_{cc1} - 2))^2 - \varepsilon_{c1}^2\varepsilon_c^2(E_{cc1} - 2)^2$$
$$(E_{cc1} - 1)^2(12X^3 h\cos(\beta) + 6X^2 h^2\cos(\beta)^2) + \varepsilon_c^4(E_{cc1} - 2)^4(4Xh^3\cos(\beta)^3$$
$$-3h^4\cos(\beta)^4) + 12X^3\varepsilon_{c1}^3 h\cos(\beta)\varepsilon_c(E_{cc1} - 2)(E_{cc1} - 1)^2 + 4h^3\cos(\beta)^3\varepsilon_c^3$$
$$X\varepsilon_{c1}(E_{cc1} - 2)^3(E_{cc1} - 1)^2)/k15$$

$$k10 = 6\varepsilon_{c1}^2\varepsilon_c(E_{cc1}-1)^2(E_{cc1}-2)(X^2 b\sin(\beta)-X^3(1-k6+k2))+3\varepsilon_{c1}\varepsilon_c^2$$
$$(E_{cc1}-1)^2(E_{cc1}-2)^2(X^3-Xb^2\sin(\beta)^2)+6\varepsilon_{c1}^3X^3(E_{cc1}-1)^2(k2-k6)$$
$$+\varepsilon_c^3(E_{cc1}-2)^3(X^3+2b^3\sin(\beta)^3-3Xb^2\sin(\beta)^2)$$

$$k11 = (12X^4(k1-k6)(E_{cc1}-1)^2\varepsilon_{c1}^2(\varepsilon_{c1}-\varepsilon_c(E_{cc1}-2))^2-\varepsilon_{c1}^2\varepsilon_c^2(E_{cc1}-2)^2$$
$$(E_{cc1}-1)^2(12X^3b\sin(\beta)+6X^2b^2\sin(\beta)^2)+\varepsilon_c^4(E_{cc1}-2)^4(4Xb^3\sin(\beta)^3$$
$$-3b^4\sin(\beta)^4)+12X^3\varepsilon_{c1}^3b\sin(\beta)\varepsilon_c(E_{cc1}-2)(E_{cc1}-1)^2+4b^3\sin(\beta)^3\varepsilon_c^3$$
$$X\varepsilon_{c1}(E_{cc1}-2)^3(E_{cc1}-1)^2)/k15$$

$$k12 = 6\varepsilon_{c1}^2\varepsilon_c(E_{cc1}-1)^2(E_{cc1}-2)(X^2 b\sin(\beta)-X^3(1-k7+k2))+3\varepsilon_{c1}\varepsilon_c^2$$
$$(E_{cc1}-1)^2(E_{cc1}-2)^2(X^3-Xb^2\sin(\beta)^2)+6\varepsilon_{c1}^3X^3(E_{cc1}-1)^2(k2-k7)$$
$$+\varepsilon_c^3(E_{cc1}-2)^3(X^3+2b^3\sin(\beta)^3-3Xb^2\sin(\beta)^2)$$

$$k13 = (12X^4(k3-k7)(E_{cc1}-1)^2\varepsilon_{c1}^2(\varepsilon_{c1}-\varepsilon_c(E_{cc1}-2))^2-\varepsilon_{c1}^2\varepsilon_c^2(E_{cc1}-2)^2$$
$$(E_{cc1}-1)^2(12X^3b\sin(\beta)+6X^2b^2\sin(\beta)^2)+\varepsilon_c^4(E_{cc1}-2)^4(4Xb^3\sin(\beta)^3$$
$$-3b^4\sin(\beta)^4)+12X^3\varepsilon_{c1}^3b\sin(\beta)\varepsilon_c(E_{cc1}-2)(E_{cc1}-1)^2+4b^3\sin(\beta)^3\varepsilon_c^3$$
$$X\varepsilon_{c1}(E_{cc1}-2)^3(E_{cc1}-1)^2)/k15$$

$$k14 = X\varepsilon_{c1}\varepsilon_c^2(E_{cc1}-2)^4\sin(\beta)\cos(\beta)$$

$$k15 = k14\varepsilon_c(E_{cc1}-2)$$

ANNEX II

The strains, in each side of the section referenced in Fig. 7, have a linear variation between the extreme values ε_1 and ε_2, given by the following expressions:

$$\textit{Side } 1 \begin{cases} \varepsilon_1 = \varepsilon_c - \dfrac{\varepsilon_c}{X}((b-a)\sin\beta + a\cos\beta) \\ \varepsilon_2 = \varepsilon_c - \dfrac{\varepsilon_c}{X}((h-a)\cos\beta + (b-a)\sin\beta) \end{cases}$$

$$Side\ 2 \begin{cases} \varepsilon_1 = \varepsilon_c - \dfrac{\varepsilon_c}{X} a(\sin\beta + \cos\beta) \\ \varepsilon_2 = \varepsilon_c - \dfrac{\varepsilon_c}{X}((b-a)\sin\beta + a\cos\beta) \end{cases}$$

$$Side\ 3 \begin{cases} \varepsilon_1 = \varepsilon_c - \dfrac{\varepsilon_c}{X} a(\sin\beta + \cos\beta) \\ \varepsilon_2 = \varepsilon_c - \dfrac{\varepsilon_c}{X}((h-a)\cos\beta + a\sin\beta) \end{cases}$$

$$Side\ 4 \begin{cases} \varepsilon_1 = \varepsilon_c - \dfrac{\varepsilon_c}{X}((h-a)\cos\beta + a\sin\beta) \\ \varepsilon_2 = \varepsilon_c - \dfrac{\varepsilon_c}{X}((h-a)\cos\beta + (b-a)\sin\beta) \end{cases}$$

The definitions of x_{p1}, x_{p2}, H_1 to H_8 are :

$$x_{p1} = \frac{\varepsilon_1 f_{syd}\xi}{|\varepsilon_1| E_S(\varepsilon_2 - \varepsilon_1)} - \frac{(\varepsilon_2 - \varepsilon_1)\xi}{2(\varepsilon_2 - \varepsilon_1)};\ x_{p2} = \frac{\varepsilon_2 f_{syd}\xi}{|\varepsilon_2| E_S(\varepsilon_2 - \varepsilon_1)} - \frac{(\varepsilon_2 - \varepsilon_1)\xi}{2(\varepsilon_2 - \varepsilon_1)}$$

$$H_1 = Heaviside\left(\varepsilon_1 - \frac{f_{syd}}{E_s}\right);\ H_2 = Heaviside\left(\varepsilon_2 - \frac{f_{syd}}{E_s}\right)$$

$$H_3 = Heaviside\left(\varepsilon_1 + \frac{f_{syd}}{E_s}\right);\ H_4 = Heaviside\left(\varepsilon_2 + \frac{f_{syd}}{E_s}\right)$$

$$H_5 = Heaviside\left(\frac{f_{syd}}{E_s} - \varepsilon_1\right);\ H_6 = Heaviside\left(-\frac{f_{syd}}{E_s} - \varepsilon_1\right)$$

$$H_5 = Heaviside\left(\frac{f_{syd}}{E_s} - \varepsilon_2\right);\ H_8 = Heaviside\left(-\frac{f_{syd}}{E_s} - \varepsilon_2\right)$$

The value of ξ is $\xi = h - 2a$ if the sides are 1 or 3 and $\xi = b - 2a$ if the sides are 2 or 4.
The resultant force in the steel at side i, with $i = 1$ to 4, is computed through the expression:

$$F_i = f_{syd} a_i \left\{ H_1 H_2 \xi - H_8 H_6 \xi + H_2 H_3 H_5 \left(\xi - \frac{1}{2}\left(1 - \varepsilon_1 \frac{E_S}{f_{syd}}\right)\left(\frac{\xi}{2} + x_{p2}\right)\right) + \right.$$

$$\left. + \left(\frac{\varepsilon_1 f_{syd}\xi}{|\varepsilon_1| E_s(\varepsilon_2 - \varepsilon_1)} + x_{p2} \right)(H_1 H_8 - H_2 H_6) + H_4 H_6 H_7 \right.$$

$$\left(\frac{1}{2}\left(1 + \varepsilon_2 \frac{E_s}{f_{syd}}\right)\left(\frac{\xi}{2} - x_{p1}\right) - \xi \right)$$

$$-H_8 H_3 H_5 \left(\xi - \frac{1}{2}\left(1 + \varepsilon_1 \frac{E_s}{f_{syd}}\right)\left(\frac{\xi}{2} + x_{p2}\right)\right) + H_1 H_4 H_7 \left(\xi + \frac{1}{2}\left(-1 + \varepsilon_2 \frac{E_s}{f_{syd}}\right)\left(\frac{\xi}{2} - x_{p1}\right)\right)\Bigg\}$$

$$+\frac{1}{2} H_3 H_5 H_4 H_7 E_s (\varepsilon_1 + \varepsilon_2) \xi \; a_i$$

The bending moment dF_i at side i, with $i = 1$ to 4, is given by:

$$dF_i = \frac{1}{6} H_3 H_5 \left(\frac{\xi}{2} + x_{p2}\right)(\xi - x_{p2})((f_{syd} + \varepsilon_1 E_s) H_8 - (f_{syd} - \varepsilon_1 E_s) H_2) a_i +$$

$$+\frac{1}{2}\left[\frac{\xi^2}{2} - (x_{p2})^2 - (x_{p1})^2 + \frac{1}{3}(x_{p2} - x_{p1})^2\right](H_8 H_1 - H_2 H_6) f_{syd} \; a_i$$

$$+\frac{1}{6} H_4 H_7 \left(\frac{\xi}{2} - x_{p1}\right)(\xi + x_{p1})((f_{syd} - \varepsilon_2 E_s) H_1 - (f_{syd} + \varepsilon_2 E_s) H_6) a_i +$$

$$+\frac{1}{2} H_3 H_5 H_4 H_7 (\varepsilon_1 + \varepsilon_2)\left(\frac{\xi}{2} - \frac{\xi(\varepsilon_1 + 2\varepsilon_2)}{3\varepsilon_1 + 3\varepsilon_2}\right) \xi \; E_s \; a_i$$

NB